ISBN: 978-3-95450-227-1 ISSN: 2673-5490 doi:10.18429/JACoW-IPAC2022-MOPOST035

OPERATIONAL EXPERIENCE AND PERFORMANCE OF THE REX/HIE-ISOLDE LINAC

J.A Rodriguez†, N. Bidault, E. Fadakis, P. Fernier, M. Lozano Benito, S. Mataguez, E. Piselli, E. Siesling, CERN, Geneva, Switzerland

Abstract

Located at CERN, ISOLDE is one of the world's leading research facilities in the field of nuclear science. Radioactive Ion Beams (RIBs) are produced when 1.4 GeV protons transferred from the Proton Synchrotron Booster (PSB) to the facility impinge on one of the two available targets. The RIB of interest is extracted, mass-separated and transported to one of the experimental stations, either directly, or after being accelerated in the REX/HIE-ISOLDE post-accelerator. In addition to a Penning trap (REXTRAP) to accumulate and transversely cool the beam and a charge breeder (REXEBIS) to boost the charge state of the ions, the post-accelerator includes a linac with both room temperature (REX linac) and superconducting (HIE-ISOLDE linac) sections followed by three HEBT lines to deliver the beam to the different experimental stations. The latest upgrades of the facility as well as a comprehensive list of the RIBs delivered to the users of the facility and the operational experience gained during the last physics campaigns will be presented in this contribution.

THE REX/HIE-ISOLDE LINAC

The REX linac consists of seven room temperature accelerating structures (Fig. 1). A four-rod RFQ followed by a buncher, an IH structure, three spiral resonators and a second IH structure accelerate the beam from an injection energy of 5 keV/u to 2.8 MeV/u [1]. REX is a 101.28 MHz pulsed machine with a maximum repetition rate of 50 Hz and 2 ms RF pulse length. However, it is generally operated at lower duty cycles (typically 1.0-1.6 ms pulses at 2-25 Hz depending on the optimum breeding time of the particular RIB). It is capable of accelerating beams with mass to charge ratios (A/q) between 2.5 and 4.5.

The HIE-ISOLDE linac [2] is the superconducting extension of the REX room temperature linac. It consists of four cryomodules and the corresponding inter-tank sectors. Each cryomodule is equipped with a superconducting solenoid and five superconducting Quarter Wave Resonators (QWR) made of a copper substrate coated with niobium. The geometrical beta of the QWRs is 0.103 and the maximum gradient is 6 MV/m with a nominal quality factor higher than $5 \cdot 10^8$. The final energy of the beam (Fig. 2) depends on its A/q since each QWR can be phased independently (e.g. 9.2 MeV/u for A/q = 4.5 if all QWRs could be operated at 6 MV/m).

Three HEBT lines are used to deliver the beam to different experimental stations: the Miniball spectrometer, the ISOLDE Solenoid Spectrometer (ISS) and the Scattering Chamber (SEC). The latter is occasionally replaced by different travelling experimental stations increasing the flexibility of the facility.

The diagnostic boxes (DB), distributed along the linac and HEBT lines, are equipped with Faraday cups, scanning slits, collimators, silicon detectors, beam attenuators and carbon stripping foils (50 and 75 ug/cm^2).

Electrostatic quadrupoles (before the RFQ), superconducting solenoids (inside the cryomodules) and magnetic quadrupoles (in the rest of the linac and HEBT lines) are used for transverse focusing. Two 45 deg. dipoles in each of the HEBT lines can be used as spectrometers to measure

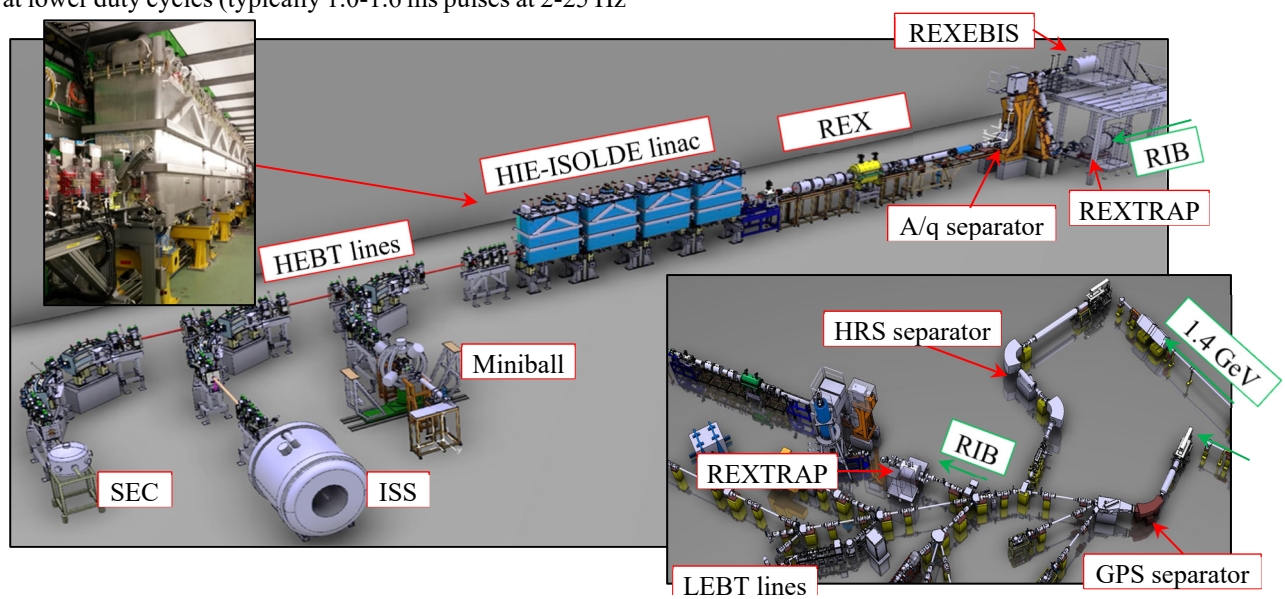

Figure 1: Layout of the ISOLDE separators and LEBT lines (bottom right) and the REX/HIE-ISOLDE post-accelerator.

† alberto.rodriguez@cern.ch

ISBN: 978-3-95450-227-1 ISSN: 2673-5490 doi:10.18429/JACoW-IPAC2022-MOPOST035

the beam energy and to clean the unwanted charge states of beam contaminants when stripping foils are used.

Table 1: List of post-accelerated RIBs since 2015. The duration of each experiment and a reference to the experimental proposal with additional information is included.

Beam(s)	Energies [MeV/u]	Time [hrs]	Exp. number
$^{74}Zn^{21,25+}$, $^{76}Zn^{22+}$	2.8, 4.0	~ 170	IS557 [3]
$^{110}Sn^{26+}$	4.5	115	IS562 [4]
$^{142}Xe^{33+}$	4.5	100	IS548 [5]
$^{78}Zn^{20+}$	4.3	130	IS557 [3]
$^{132}Sn^{31+}$	5.5	130	IS551 [6]
$^{9}Li^{3+\rightarrow3+}$	6.8	70	IS561 [7]
$^{66}Ni^{16+}$	4.5	140	IS559 [8]
$^{72}Se^{19+}$	4.4	33	IS597 [9]
$^{66}Ge^{17+}$, $^{70}Se^{16+}$	4.4	97	IS569 [10]
$^{142}Ba^{33+}$, $^{144}Ba^{33+}$	3.4, 4.2	147	IS553 [11]
$^{140}Sm^{34+}$	4.7	113	IS558 [12]
$^{15}C^{5+\rightarrow6+}$	4.4	245	IS619 [13]
$^{94}Rb^{23+}$	6.2	140	IS572 [14]
$^{142}Sm^{33+}$, $^{140}Nd^{33+}$	4.6	166	IS546 [15]
$^{108}Sn^{26+}$	4.5	94	IS562 [4]
$^{9}Li^{3+\rightarrow3+}$	8.0	80	IS561 [7]
$^{206}Hg^{46+}$	4.2	84	IS547 [16]
$^{59}Cu^{20+}$	3.6, 4, 5, 4.3, 4.7	134	IS607 [17]
$^{28}Mg^{9+}$	5.5	176	IS628 [18]
$^{96}Kr^{23+}$	4.7, 5.3	178	IS644 [19]
$^{212}Rn^{50+}$	3.8, 4.4	49	IS506 [20]
$^{222}Ra^{51+}$, $^{228}Ra^{53+}$	4.3	31,	IS552 [21]
$^{224,226}Rn^{52+}$, $^{222}Rn^{51+}$	4.2, 5.1	83	
$^{142}Ba^{33+}$	4.2	39	IS553 [11]
$^{106}Sn^{26+}$	4.4	91	IS562 [4]
$^{8}B^{3+\rightarrow5+}$	4.9	97	IS616 [22]
$^{11}Be^{4+\rightarrow4+}$	7.5	118	IS629 [23]
$^{134,132}Sn^{31+}$	7.4, 7.2	68	IS654 [24]
$^{28}Mg^{9+}$	9.5	116	IS651 [25]
$^{28}Mg^{9+}$	9.5	117	IS621 [26]
$^{206}Hg^{46+}$	7.4	98	IS631 [27]
$^{9}Li^{3+\rightarrow3+}$	8.0	103	IS561 [7]
$^{7}Be^{2+\rightarrow4+}$	5.0	135	IS554 [28]
$^{30}Mg^{11+}$	8.5	~ 150	IS680 [29]
$^{212}Rn^{50+}$	7.6	~ 150	IS689 [30]
$^{61}Zn^{16+}$	7.5	~ 150	IS675 [31]
$^{209}Fr^{53+}$	7.6	~ 110	IS581 [32]

OPERATIONAL EXPERIENCE

The HIE-ISOLDE project was phased over four years. A new cryomodule was installed every year between 2015 and 2018 [33,34]. High-energy physics campaigns started right after the commissioning of each cryomodule was completed. Physics was paused in 2019 and 2020 during CERN's Long Shutdown 2 (LS2) and restarted in 2021.

The diversity of beams delivered to the users of the facility (Table 1) demonstrates the flexibility of the REX/HIE-ISOLDE linac. Isotopes as light as ^{8}B and as heavy as ^{228}Ra, with beam energies as high as 9.5 MeV/u for ^{28}Mg or 1.6 GeV for ^{212}Rn, multiple production target materials, ionization schemes (surface, plasma and laser) and mass-separators have been used over the years.

PERFORMANCE

The REX/HIE-ISOLDE linac reliably delivers the beams requested by the users of the facility. The beam availability is ~ 90-95 %. The main sources of downtime are: issues in the proton injector chain (i.e. linac4 and PSB) accounting for ~1-3 % downtime, issues with the ISOLDE targets, separators and LEBT lines for ~2-3 % and trips of the linac RF systems for ~2-4 % (roughly evenly split between room temperature and superconducting systems).

Beam Intensity

Even if it is not part of the performance of the linac itself, several experiments were not able to achieve some of their physics goals due to lower than anticipated beam intensities. Sustaining the required target production during the duration of an experiment (typically 3-8 days) was especially challenging when molecular beams were used to limit isobaric beam contaminants ($^{8}B^{19}F_2^{+}$ for IS616, $^{134}Sn^{34}S^{+}$ for IS654 or $^{70,72}Se^{12}C^{16}O^{+}$ for IS597 and IS569).

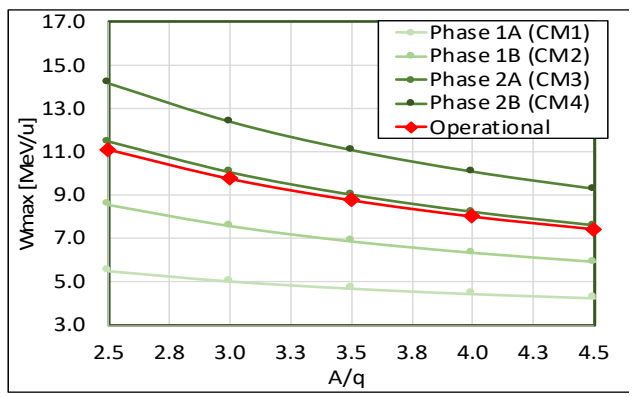

Figure 2: REX/HIE-ISOLDE nominal and operational maximum beam energy for mass to charge ratio.

Beam Energy

On average, the operational gradient of the SRF cavities has been limited to ~75 % of the nominal 6 MV/m (Fig. 2). The RF coupler of one of the cavities was damaged and the cavity was unusable until it was repaired during the LS2. Several cavities suffer from field emission and they have to be operated at a lower gradient to limit the thermal load

ISBN: 978-3-95450-227-1 ISSN: 2673-5490 doi:10.18429/JACoW-IPAC2022-MOPOST035

in the cryoplant and to avoid damaging the instrumentation with the produced X-rays. A few additional cavities are not stable enough for operation at high fields due to a mechanical instability thought to be generated in the cryo system and propagated through the LHe bath. Fortunately, the 75 % limitation in total gradient did not impact the physics program significantly up to now (except for part of experiment IS631: $^{206}Hg^{46+}$ at 10 MeV/u requested vs. 9.4 MeV/u delivered). Nevertheless, higher beam energies will not be reachable until these issues are addressed.

Stability, Scalability and Reproducibility

In general, the linac only requires minor adjustments when it is scaled over $\Delta(A/q) < \pm 0.2$ which is critical for RIBs machines. Scaling constraints are more evident when the final A/q approaches 4.5 because of the limited available RF power and focusing strength of the in-vacuum triplet inside the first IH structure. In addition, one of the spiral resonators suffers from a mechanical instability at high gradients which limits its scalability. To avoid this problem, and until the source of the issue is identified and corrected, this structure is being operated at a lower gradient than nominal which temporarily limits the final energy of REX to 2.75 MeV/u (instead of 2.8 MeV/u).

Beam Transmission and Ionization Efficiencies

Transmission through the separators and LEBT lines is typically ~ 70 % (up to 80 % if enough time is invested in the preparation of the set-up). Transmission through the linac and HEBT lines is usually ~ 75 %. Beam losses are dominated by the intrinsic inefficiency of the bunching process of the RFQ. Trapping and ionization efficiencies of the REXTRAP and the REXEBIS vary significantly (typically 2-12 %) depending on the type of beam (atomic vs. molecular), the mass and atomic number of the isotope, the desired charge state and the beam intensity among others [35].

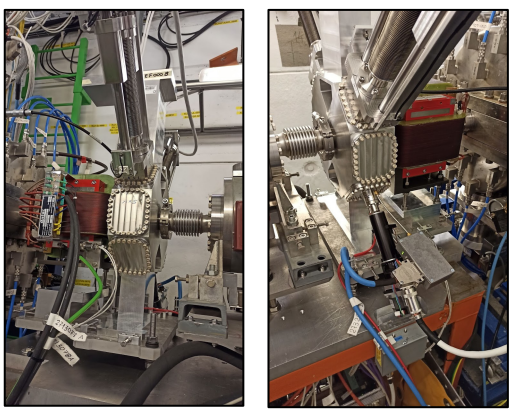

Figure 3: Recently installed horizontal/vertical steerers and beam instrumentation boxes in the REX linac.

Duration of the Experimental Campaigns

The required maintenance of the cryoplant imposes scheduling constraints to the high-energy physics campaigns. In contrast to other post-accelerated RIB facilities, the cryomodules need to be warmed up and cooled down every year. This cycle, together with the required conditioning and recommissioning of the SRF cavities that follows, takes several months. The high-energy physics campaign typically starts as soon as the beam recommissioning is completed in mid-July and it ends when the injectors stop delivering protons in November.

Beam Instrumentation

The beam instrumentation of the REX linac was recently consolidated. Three new diagnostic boxes (Fig. 3) are now fully operational. Thanks to the new instrumentation and a new horizontal/vertical steerer, losses in the linac have been reduced by ~ 10 %. Silicon detectors have demonstrated their value to characterize both the transverse and longitudinal space of very low-intensity beams, common in RIB facilities [36]. Hence, several additional ones have been installed in the HIE-ISOLDE linac and HEBT lines over the years.

CONCLUSION

The REX/HIE-ISOLDE linac has reliably delivered dozens of RIBs to the users of the facility since 2016. However, in order to maintain the 90-95 % machine availability in the future, the REX RF systems (particularly the aging amplifiers and LLRF) will need to be consolidated. Reaching the nominal accelerating gradient of the SRF cavities as well as extending the physics campaign beyond the current four months per year remain a priority for the user community and will be necessary to keep the facility competitive in the global context.

ACKNOWLEDGEMENTS

The authors (and the users of the facility) would like to thank the technical teams at CERN for their commitment to ISOLDE and invaluable support during the commissioning and operation of the post-accelerator.

REFERENCES

[1] F. Ames *et al.,* “The REX-ISOLDE Facility: Design and Commissioning Report”, CERN, Geneva, Switzerland, Rep. CERN-2005-009, Sep. 2005.

[2] Y. Kadi *et al.*, “HIE-ISOLDE – Technical Design Report for the Energy Upgrade”, CERN, Geneva, Switzerland, Rep. CERN-2018-002-M, May 2018.| doi: 10.23731/CYRM-2018-001

[3] E. Rapisarda *et al.,* “Coulomb excitation 74Zn-80Zn (N=50): probing the validity of shell-model descriptions around 78Ni”, IS557, Rep. INTC-P-353, Oct. 2012.

[4] J. Cederkall *et al.*, “Transfer Reactions and Multiple Coulomb Excitation in the 100Sn Region”, IS562, INTC-P-362, Rep. CERN-INTC-2012-061, Oct. 2012.

[5] T. Kroll *et al.*, “Evolution of quadrupole and octupole collectivity north-east of 132Sn: the even Te and Xe isotopes”, IS548, INTC-P-342, Rep. CERN-INTC-2012-041, Oct. 2012.

[6] P. Reiter *et al.*, “Coulomb excitation of doubly magic 132Sn with MINIBALL at HIE-ISOLDE”, IS551, INTC-P-345, Rep. CERN-INTC-2012-044, Oct. 2012.

ISBN: 978-3-95450-227-1 ISSN: 2673-5490 doi:10.18429/JACoW-IPAC2022-MOPOST035

[7] K. Riisager *et al.*, "Transfer reactions at the neutron dripline with triton target", IS561, INTC-P-361, Rep. CERN-INTC-2012-060, Oct. 2012.

[8] S. Siem *et al.*, "Statistical properties of warm nuclei: Investigating the low-energy enhancement in the gamma strength function of neutron-rich nuclei", IS559, INTC-P-355, Rep. CERN-INTC-2012-054, Oct. 2012.

[9] D. T. Doherty *et al.*, "Probing Shape Coexistence in neutron-deficient 72Se via Low-Energy Coulomb Excitation", IS597, INTC-P-423, Rep. CERN-INTC-2014-057, Oct. 2014.

[10] N. Orce *et al.*, "Solving the shape conundrum in 70Se", IS569, INTC-P-368, Rep. CERN-INTC-2012-067, Oct. 2012.

[11] M. Scheck *et al.*, "Determination of the B(E3,0+→3−) strength in the octupole-correlated nuclei 142, 144 Ba using Coulomb excitation", IS553, INTC-P-348, Rep. CERN-INTC-2012-047, Oct. 2012.

[12] A. Gorgen *et al.*, "Shape Transition and Coexistence in Neutron-Deficient Rare Earth Isotopes", IS558, INTC-P-354, Rep. CERN-INTC-2012-053, Oct. 2012.

[13] I. Martel *et al.*, "Effects of the neutron halo in 15C scattering at energies around the Coulomb barrier", IS619, INTC-P-468, Rep. CERN-INTC-2016-025, May 2016.

[14] J.J. Valient Dobon *et al.*, "Study of shell evolution around the doubly magic 208Pb via a multinucleon transfer reaction with an unstable beam", IS572, INTC-P-379, Rep. CERN-INTC-2013-015, May 2013.

[15] C. Bauer *et al.*, "Study of the effect of shell stabilization of the collective isovector valence-shell excitations along the N=80 isotonic chain", IS546, INTC-P-339, Rep. CERN-INTC-2012-038, Oct. 2012.

[16] Z. Podolyak *et al.*, "Coulomb excitation of the two proton-hole nucleus 206Hg", IS547, INTC-P-340, Rep. CERN-INTC-2012-039, Sep. 2012.

[17] C. Lederer *et al.*, "The 59Cu(p,alpha) cross section and its implications for nucleosynthesis in core collapse supernovae", IS607, INTC-P-441, Rep. CERN-INTC-2015-036, Jun. 2015.

[18] G. Georgiev *et al.*, "Nuclear moment studies of short-lived excited states towards the Island of Inversion. g factor of 28Mg (2+) using TDRIV on H-like ions", IS628, INTC-P-478, Rep. CERN-INTC-2016-047, Oct. 2016.

[19] K. Moschner *et al.*, "A Coulomb-nuclear excitation study of shape co-existence in 96Kr", IS644, Rep. CERN-INTC-2017-062, INTC-P-517, May 2017.

[20] T. Grahn *et al.*, "Mapping the boundaries of the seniority regime and collective motion: Coulomb excitation studies of N = 122 isotones 206Po and 208Rn", IS506, INTC-P-284, Rep. CERN-INTC-2010-068, Oct. 2010.

[21] P. Butler *et al.*, "Measurements of octupole collectivity in Rn and Ra nuclei using Coulomb excitation", IS552, INTC-P-347-ADD-1, Rep. CERN-INTC-2013-019, Sep. 2013.

[22] A. Di Pietro *et al.*, "Reaction mechanisms in collisions induced by 8B beam close to the barrier", IS616, INTC-P-463, Rep. CERN-INTC-2016-018, Jan. 2016

[23] C. Mazzocchi *et al.*, "Beta decay of 11Be", IS629, INTC-P-479, Rep. CERN-INTC-2016-048, Oct. 2016.

[24] T. Kroell *et al.*, "First spectroscopy of the the r-process nucleus 135Sn", IS654, INTC-P-539, Rep. CERN-INTC-2018-008, Jan. 2018.

[25] D. Muecher *et al.*, "Nuclear Shell Evolution in the Island of Inversion Studied via the 28 Mg(t, 30 Mg)p reaction", IS651, INTC-CLL-036, Rep. CERN-INTC-2017-090, Oct. 2017.

[26] D. Sharp *et al.*, "Single-particle behaviour towards the island of inversion - 28,30Mg(d,p)29,31Mg in inverse kinematics", IS621, INTC-P-470, Rep. CERN-INTC-2016-030, Jun. 2016.

[27] B.P. Kay *et al.*, "The (d,p) reaction on 206Hg", IS631, INTC-CLL-026, Rep. CERN-INTC-2016-056, Oct, 2016.

[28] D. Gupta *et al.*, "Search for higher excited states of 8Be* to study the cosmological 7Li problem", IS554, INTC-P-350, Rep. CERN-INTC-2012-049, Oct. 2012.

[29] D. Sharp *et al.*, "The d(30Mg,p)31Mg reaction: Probing single-particle behaviour within the "island of inversion", IS680, INTC-P-576, Rep. CERN-INTC-2020-060, Sep. 2020.

[30] D. Sharp *et al.*, "Evolution of single-particle states along N=127: The d(212Rn,p)213Rn reaction", IS689, INTC-P-594, Rep. CERN-INTC-2021-010, Jan. 2021.

[31] G. Lotay *et al.*, "Investigating the key rp process reaction 61Ga(p,γ)62Ge reaction via 61Zn(d,p)62Zn transfer", IS675, INTC-P-570, Rep. CERN-INTC-2020-053, Sep. 2020.

[32] M. Veselsky *et al.*, "Determination of the fission barrier height in fission of heavy radioactive beams induced by the (d,p)-transfer", IS581, INTC-P-356, Rep. CERN-INTC-2012-055, Oct. 2012.

[33] J.A. Rodriguez *et al.*, "First Operational Experience of HIE-ISOLDE", presented at IPAC'16, paper TUPMR023.

[34] J.A. Rodriguez *et al.*, "Beam Commissioning of the HIE-ISOLDE Post-Accelerator", presented at IPAC'16, paper WEOBA01.

[35] H. Pahl *et al.*, "Nonadiabatic electron gun at an electron beam ion source: Commissioning results and charge breeding investigations", Physical Review Accelerators and Beams, vol. 25, p. 013402, Jan. 2022. doi:10.1103/PhysRevAccelBeams.25.013402

[36] N. Bidault, "Characterization of Very Low Intensity Ion Beams from the REX/HIE-ISOLDE Linear Accelerator at CERN", Ph.D. thesis, Sapienza Universita di Roma, Rome, Italy, 2021